

Supplementary Material for:  
Scaling Towards the Critical Point in the Combined  
Reaction/Gibbs Ensemble

H. Mert Polat<sup>a</sup>, Silvia Lasala<sup>b</sup>, Frédérick de Meyer<sup>c,d</sup>, Céline Houriez<sup>d</sup>,  
Othonas A. Moulton<sup>a</sup>, Thijs J. H. Vlugt<sup>a,\*</sup>

<sup>a</sup>*Engineering Thermodynamics, Process & Energy Department, Faculty of Mechanical Engineering, Delft University of Technology, Leeghwaterstraat 39, Delft 2628CB, The Netherlands*

<sup>b</sup>*Université de Lorraine, Laboratoire Réactions et Génie des Procédés, 54000 Nancy, France*

<sup>c</sup>*CO<sub>2</sub> and Sustainability R&D Program, Gas & Low Carbon Entity, OneTech, TotalEnergies S.E., 92078 Paris, France*

<sup>d</sup>*Mines Paris, PSL University, Center for Thermodynamics of Processes (CTP), 77300 Fontainebleau, France*



---

\*Corresponding author

*Email address:* [t.j.h.vlugt@tudelft.nl](mailto:t.j.h.vlugt@tudelft.nl) (Thijs J. H. Vlugt)

Table S1: Values of  $\ln \left[ \frac{q_i}{\Lambda_i^3 \rho_0} \right]$  for monomer ( $\text{NO}_2$  or A) and dimer ( $\text{N}_2\text{O}_4$  or  $\text{A}_2$ ), and natural logarithms of ideal gas reaction equilibrium constants ( $\ln[K_{\text{IG}}]$ ) as a function of temperature for reaction R1 of the main text for systems 1, 2, and 3. The values of  $\ln \left[ \frac{q_i}{\Lambda_i^3 \rho_0} \right]$  as a function temperature are calculated using the correlation reported by Lasala et al. [1] (Eqs. 10 and 11 of the main text). The ideal gas reaction equilibrium constants for reaction R1 are computed using Eq. 9 of the main text.

$T / [\text{K}]$	$\ln \left[ \frac{q_i}{\Lambda_i^3 \rho_0} \right]$		$\ln[K_{\text{IG}}]$
	Monomer	Dimer	
180	632.98	1293.17	27.21
190	600.53	1226.33	25.28
200	571.32	1166.17	23.53
210	544.90	1111.75	21.95
220	520.87	1062.27	20.52
230	498.94	1017.09	19.21
240	478.83	975.68	18.01
250	460.34	937.58	16.91
260	443.26	902.41	15.89
270	427.45	869.85	14.94
275	419.98	854.46	14.50
280	412.77	839.61	14.07
290	399.10	811.46	13.25
300	386.35	785.19	12.49
310	374.41	760.61	11.78
320	363.23	737.56	11.11
330	352.72	715.92	10.48
340	342.83	695.54	9.89
350	333.50	676.33	9.34
360	324.69	658.19	8.81
370	316.36	641.03	8.31
380	308.46	624.77	7.84
390	300.98	609.35	7.39
395	297.37	601.93	7.18
400	293.86	594.69	6.97
405	290.44	587.64	6.77
410	287.09	580.75	6.57
415	283.83	574.04	6.37

Table S2: Values of  $\ln \left[ \frac{q_i}{\Lambda_i^3 \rho_0} \right]$  for monomer and dimer, and natural logarithms of ideal gas reaction equilibrium constants ( $\ln[K_{\text{IG}}]$ ) as a function of temperature for reaction R1 of the main text for system 4. Lasala et al. [1] reported two correlations to calculate the isolated molecule partition functions of  $\text{N}_2\text{O}_4$  and  $\text{NO}_2$  (Eqs. 10 and 11 of the main text, respectively). We modified the values computed using the correlations from Lasala et al. [1] by decreasing the isolated molecule partition functions of  $\text{N}_2\text{O}_4$  by  $10 \ln \left[ \frac{q_i}{\Lambda_i^3 \rho_0} \right]$  units for each temperature. The ideal gas reaction equilibrium constants for reaction R1 are computed using Eq. 9 of the main text.

$T / [\text{K}]$	$\ln \left[ \frac{q_i}{\Lambda_i^3 \rho_0} \right]$		$\ln[K_{\text{IG}}]$
	Monomer	Dimer	
180	632.98	1283.17	17.21
190	600.53	1216.33	15.28
200	571.32	1156.17	13.53
210	544.90	1101.75	11.95
220	520.87	1052.27	10.52
230	498.94	1007.09	9.21
240	478.83	965.68	8.01
250	460.34	927.58	6.91
260	443.26	892.41	5.89
270	427.45	859.85	4.94
275	419.98	844.46	4.50
280	412.77	829.61	4.07
290	399.10	801.46	3.25
300	386.35	775.19	2.49
310	374.41	750.61	1.78
320	363.23	727.56	1.11
330	352.72	705.92	0.48
340	342.83	685.54	-0.11
350	333.50	666.33	-0.66
360	324.69	648.19	-1.19
370	316.36	631.03	-1.69
380	308.46	614.77	-2.16
390	300.98	599.35	-2.61
395	297.37	591.93	-2.82
400	293.86	584.69	-3.03
405	290.44	577.64	-3.23
410	287.09	570.75	-3.43
415	283.83	564.04	-3.63

Table S3: Values of  $\ln \left[ \frac{q_i}{\Lambda_i^3 \rho_0} \right]$  for monomer and dimer, and natural logarithms of ideal gas reaction equilibrium constants ( $\ln[K_{\text{IG}}]$ ) as a function of temperature for reaction R1 of the main text for system 5. Lasala et al. [1] reported two correlations to compute the isolated molecule partition functions of  $\text{N}_2\text{O}_4$  and  $\text{NO}_2$  (Eqs. 10 and 11 of the main text, respectively). We scaled up the values of isolated molecule partition functions of  $\text{N}_2\text{O}_4$  computed by Lasala et al. [1] by 1% for system 5. The ideal gas reaction equilibrium constants for reaction R1 are computed using Eq. 9 of the main text.

$T / [\text{K}]$	$\ln \left[ \frac{q_i}{\Lambda_i^3 \rho_0} \right]$		$\ln[K_{\text{IG}}]$
	Monomer	Dimer	
180	632.98	1306.10	40.14
190	600.53	1238.59	37.54
200	571.32	1177.84	35.19
210	544.90	1122.86	33.07
220	520.87	1072.89	31.14
230	498.94	1027.26	29.38
240	478.83	985.44	27.77
250	460.34	946.96	26.28
260	443.26	911.44	24.91
270	427.45	878.55	23.64
275	419.98	863.00	23.04
280	412.77	848.01	22.46
290	399.10	819.58	21.37
300	386.35	793.04	20.34
310	374.41	768.21	19.38
320	363.23	744.94	18.49
330	352.72	723.08	17.64
340	342.83	702.50	16.85
350	333.50	683.10	16.10
360	324.69	664.77	15.39
370	316.36	647.44	14.72
380	308.46	631.02	14.09
390	300.98	615.44	13.49
395	297.37	607.95	13.20
400	293.86	600.64	12.92
405	290.44	593.51	12.64
410	287.09	586.56	12.37
415	283.83	579.78	12.11

Table S4: Values of  $\ln \left[ \frac{q_i}{\Lambda_i^3 \rho_0} \right]$  for monomer and dimer, and natural logarithms of ideal gas reaction equilibrium constants ( $\ln[K_{\text{IG}}]$ ) as a function of temperature for reaction R1 of the main text for system 6. Lasala et al. [1] reported two correlations to compute the isolated molecule partition functions of  $\text{N}_2\text{O}_4$  and  $\text{NO}_2$  (Eqs. 10 and 11 of the main text, respectively). We scaled down the values of isolated molecule partition functions of  $\text{N}_2\text{O}_4$  computed by Lasala et al. [1] by 1% for system 6. The ideal gas reaction equilibrium constants for reaction R1 are computed using Eq. 9 of the main text.

$T / [\text{K}]$	$\ln \left[ \frac{q_i}{\Lambda_i^3 \rho_0} \right]$		$\ln[K_{\text{IG}}]$
	Monomer	Dimer	
180	632.98	1280.24	14.28
190	600.53	1214.07	13.01
200	571.32	1154.51	11.87
210	544.90	1100.63	10.84
220	520.87	1051.65	9.90
230	498.94	1006.92	9.04
240	478.83	965.92	8.25
250	460.34	928.21	7.53
260	443.26	893.39	6.86
270	427.45	861.15	6.25
275	419.98	845.91	5.95
280	412.77	831.22	5.67
290	399.10	803.35	5.14
300	386.35	777.33	4.64
310	374.41	753.00	4.17
320	363.23	730.19	3.73
330	352.72	708.76	3.32
340	342.83	688.59	2.94
350	333.50	669.57	2.57
360	324.69	651.61	2.23
370	316.36	634.62	1.90
380	308.46	618.52	1.59
390	300.98	603.25	1.30
395	297.37	595.91	1.16
400	293.86	588.75	1.02
405	290.44	581.76	0.89
410	287.09	574.95	0.76
415	283.83	568.30	0.63

Table S5: Values of  $\beta$  as a function of dimensionless enthalpy of reaction ( $\Delta_r^*H = \frac{\Delta_r H}{RT_{c, \text{monomer}}}$ ) where  $\Delta_r^*H$  is the dimensionless enthalpy of reaction,  $\Delta_r H$  is the enthalpy of reaction in real units,  $R$  is the gas constant, and  $T_{c, \text{monomer}}$  is the critical temperature of pure monomer which is 282.4 K) and pre-exponential factor for ideal gas reaction equilibrium constants ( $\ln[K_0]$ , Eq. 13 of the main text).

		$\ln[K_0]$								
		-9.59	-8.34	-7.09	-5.84	-4.59	-3.34	-2.09	-0.84	0.41
$\Delta_r^*H$	-36.24	0.279	0.284	0.283	0.283	0.281	0.282	0.286	0.280	0.279
	-33.04	0.275	0.279	0.280	0.283	0.283	0.284	0.285	0.284	0.282
	-29.85	0.274	0.279	0.279	0.280	0.281	0.282	0.282	0.281	0.282
	-26.65	0.267	0.275	0.277	0.281	0.284	0.281	0.285	0.283	0.282
	-23.46	0.256	0.268	0.276	0.277	0.279	0.283	0.281	0.283	0.281
	-20.26	0.243	0.258	0.270	0.276	0.278	0.281	0.283	0.284	0.285
	-17.07	0.224	0.248	0.260	0.272	0.278	0.282	0.281	0.283	0.283
	-34.64	0.204	0.228	0.249	0.263	0.272	0.276	0.281	0.281	0.283
	-31.44	0.191	0.208	0.230	0.250	0.263	0.273	0.279	0.282	0.279
	-28.25	0.169	0.189	0.211	0.236	0.257	0.267	0.272	0.279	0.279
	-25.06	0.143	0.173	0.194	0.217	0.238	0.255	0.270	0.276	0.278
	-21.86	0.141	0.165	0.177	0.198	0.221	0.244	0.259	0.270	0.274
	-18.67	0.122	0.149	0.168	0.196	0.205	0.227	0.246	0.261	0.269

Table S6: Values of the normalized critical temperature ( $T_c^*$ ) as a function of dimensionless enthalpy of reaction ( $\Delta_r^*H = \frac{\Delta_r H}{RT_{c,\text{monomer}}}$  where  $\Delta_r^*H$  is the dimensionless enthalpy of reaction,  $\Delta_r H$  is the enthalpy of reaction in real units,  $R$  is the gas constant, and  $T_{c,\text{monomer}}$  is the critical temperature of pure monomer which is 282.4 K) and pre-exponential factor for ideal gas reaction equilibrium constants ( $\ln[K_0]$ , Eq. 13 of the main text). The values of  $T_c^*$  are computed as  $T_c^* = T_{c,\text{mixture}}/T_{c,\text{monomer}}$  where  $T_{c,\text{mixture}}$  is the critical temperature of the reactive binary mixture.

	$\ln[K_0]$								
	-9.59	-8.34	-7.09	-5.84	-4.59	-3.34	-2.09	-0.84	0.41
-36.24	0.279	0.284	0.283	0.283	0.281	0.282	0.286	0.280	0.279
-33.04	0.275	0.279	0.280	0.283	0.283	0.284	0.285	0.284	0.282
-29.85	0.274	0.279	0.279	0.280	0.281	0.282	0.282	0.281	0.282
-26.65	0.267	0.275	0.277	0.281	0.284	0.281	0.285	0.283	0.282
-23.46	0.256	0.268	0.276	0.277	0.279	0.283	0.281	0.283	0.281
-20.26	0.243	0.258	0.270	0.276	0.278	0.281	0.283	0.284	0.285
$\Delta_r^*H$ -17.07	0.224	0.248	0.260	0.272	0.278	0.282	0.281	0.283	0.283
-34.64	0.204	0.228	0.249	0.263	0.272	0.276	0.281	0.281	0.283
-31.44	0.191	0.208	0.230	0.250	0.263	0.273	0.279	0.282	0.279
-28.25	0.169	0.189	0.211	0.236	0.257	0.267	0.272	0.279	0.279
-25.06	0.143	0.173	0.194	0.217	0.238	0.255	0.270	0.276	0.278
-21.86	0.141	0.165	0.177	0.198	0.221	0.244	0.259	0.270	0.274
-18.67	0.122	0.149	0.168	0.196	0.205	0.227	0.246	0.261	0.269

Table S7: Values of the normalized critical density ( $\rho_c^*$ ) as a function of dimensionless enthalpy of reaction ( $\Delta_r^*H = \frac{\Delta_r H}{RT_{c,monomer}}$  where  $\Delta_r^*H$  is the dimensionless enthalpy of reaction,  $\Delta_r H$  is the enthalpy of reaction in real units,  $R$  is the gas constant, and  $T_{c,monomer}$  is the critical temperature of pure monomer which is 282.4 K) and pre-exponential factor for ideal gas reaction equilibrium constants ( $\ln[K_0]$ , Eq. 13 of the main text). The values of  $\rho_c^*$  are computed as  $\rho_c^* = \rho_{c,mixture}/\rho_{c,monomer}$  where  $\rho_{c,mixture}$  and  $\rho_{c,monomer}$  are the critical densities of the reactive binary mixture and pure monomer, respectively.

	$\ln[K_0]$									
	-9.59	-8.34	-7.09	-5.84	-4.59	-3.34	-2.09	-0.84	0.41	
-36.24	1.1778	1.1756	1.1760	1.1711	1.1778	1.1808	1.1785	1.1756	1.1759	
-33.04	1.1760	1.1944	1.1794	1.1768	1.1766	1.1769	1.2159	1.1904	1.1797	
-29.85	1.1759	1.1761	1.2383	1.2119	1.1893	1.1782	1.1779	1.2612	1.2335	
-26.65	1.2057	1.1831	1.1780	1.2815	1.2492	1.2287	1.2008	1.1856	1.1745	
-23.46	1.1747	1.1763	1.1767	1.1810	1.1780	1.1769	1.1757	1.1755	1.1742	
-20.26	1.1724	1.1744	1.1743	1.1774	1.1786	1.1754	1.1761	1.1858	1.1808	
$\Delta_r^*H$ -17.07	1.1796	1.1761	1.1734	1.1777	1.1726	1.1753	1.1758	1.1850	1.1796	
-34.64	1.1750	1.1741	1.2029	1.1920	1.1851	1.1797	1.1777	1.1758	1.1753	
-31.44	1.1738	1.1741	1.1991	1.1828	1.1743	1.1729	1.2280	1.2119	1.1989	
-28.25	1.1901	1.1829	1.1792	1.1770	1.1752	1.1746	1.2255	1.1975	1.1811	
-25.06	1.1750	1.2473	1.2372	1.2243	1.2088	1.1935	1.1862	1.1822	1.1777	
-21.86	1.1773	1.2458	1.2208	1.1954	1.1804	1.2673	1.2394	1.2460	1.2331	
-18.67	1.2187	1.2025	1.1925	1.1849	1.1817	1.2673	1.2353	1.2152	1.1902	



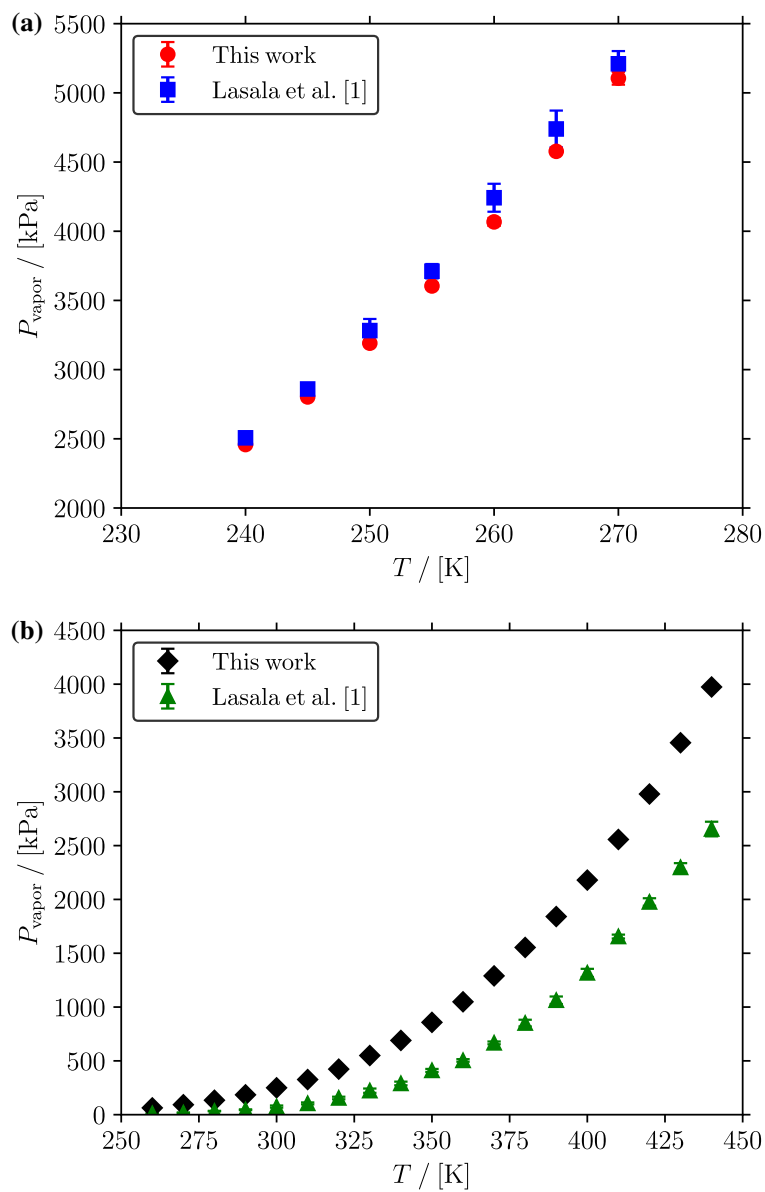


Figure S1: Comparison between the saturated vapor pressures of (a)  $\text{NO}_2$  and (b)  $\text{N}_2\text{O}_4$  computed by representing each molecule as single LJ particles (this work) and using an all-atom force field [1] as a function of temperature.

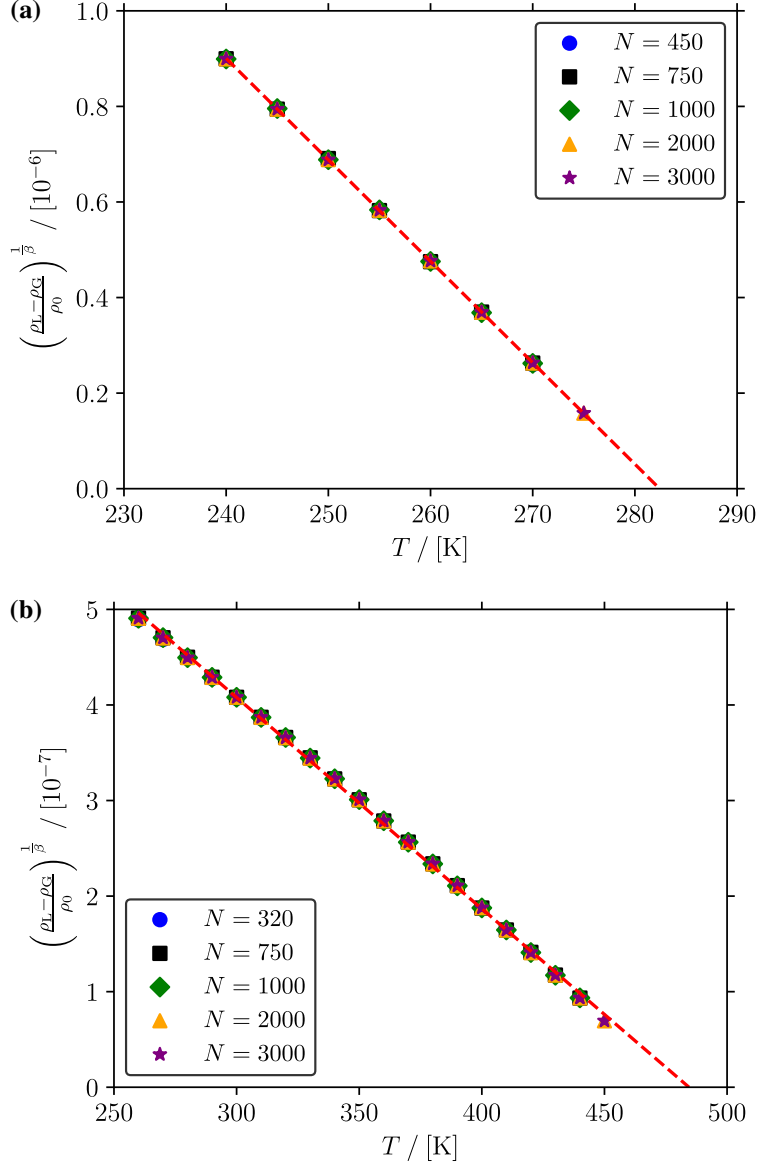


Figure S2: Values of the terms  $\left(\frac{\rho_l - \rho_g}{\rho_0}\right)^{\frac{1}{\beta}}$  ( $\beta = 0.32$ ) computed as a function of temperature for (a) pure  $\text{NO}_2$  and (b) pure  $\text{N}_2\text{O}_4$  using the force field parameters listed in Table 1 of the main text. To compute the values of  $\left(\frac{\rho_l - \rho_g}{\rho_0}\right)^{\frac{1}{\beta}}$ , we used number densities. The dashed lines represent linear regression fits to the values of  $\left(\frac{\rho_l - \rho_g}{\rho_0}\right)^{\frac{1}{\beta}}$  as a function of temperature.

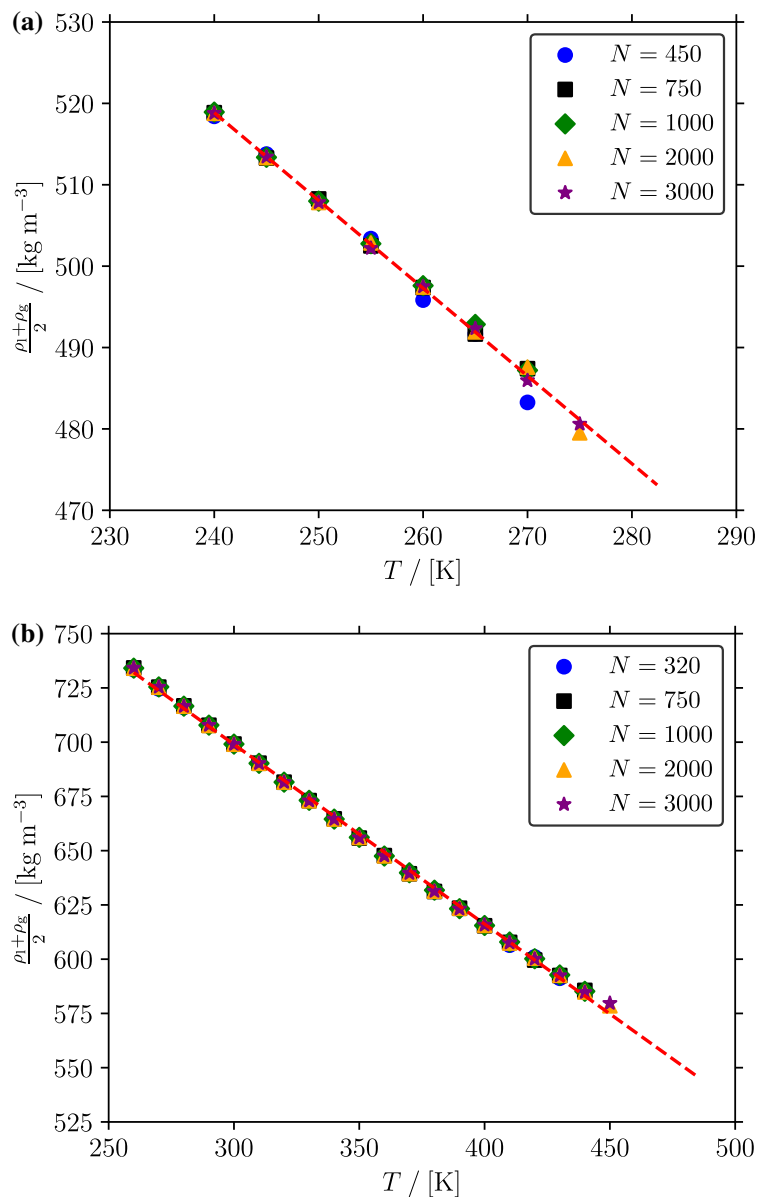


Figure S3: Average liquid and gas phase densities computed as a function of temperature for (a) pure  $\text{NO}_2$  and (b) pure  $\text{N}_2\text{O}_4$  using the force field parameters listed in Table 1 of the main text. The dashed lines represent linear regression fits to the average values of liquid and gas phase densities as a function of temperature.

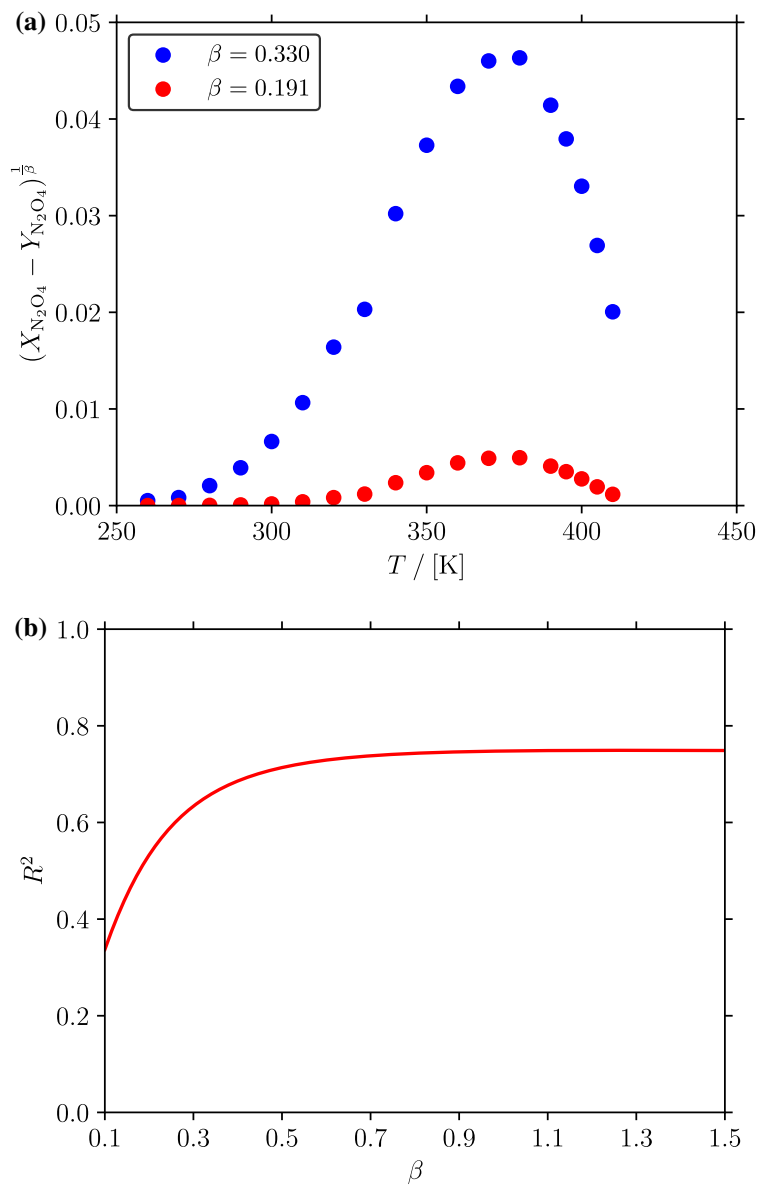


Figure S4: (a) Values of the term  $(X_i - Y_i)^{1/2}$  (see Eq. 3 of the main text) as a function of temperature for two different values of  $\beta$ , and (b) the coefficients of determination  $R^2$  of the linear regression of the values of  $(X_i - Y_i)^{1/2}$  as a function of  $\beta$  for the  $\text{NO}_2/\text{N}_2\text{O}_4$  system.

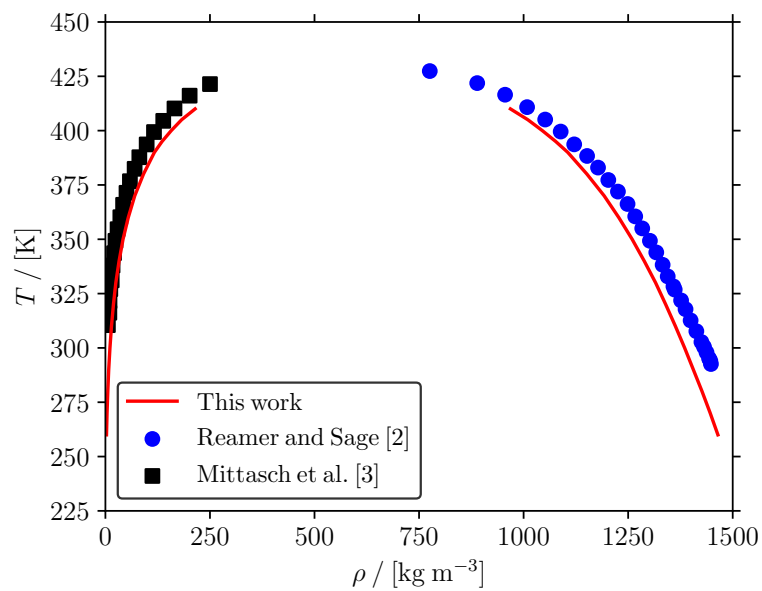


Figure S5: Comparison between the computed densities of the reactive mixture of  $\text{NO}_2$  and  $\text{N}_2\text{O}_4$  (system 1), experimental liquid densities from Reamer and Sage [2], and experimental gas densities from Mittasch et al. [3] as a function of temperature.

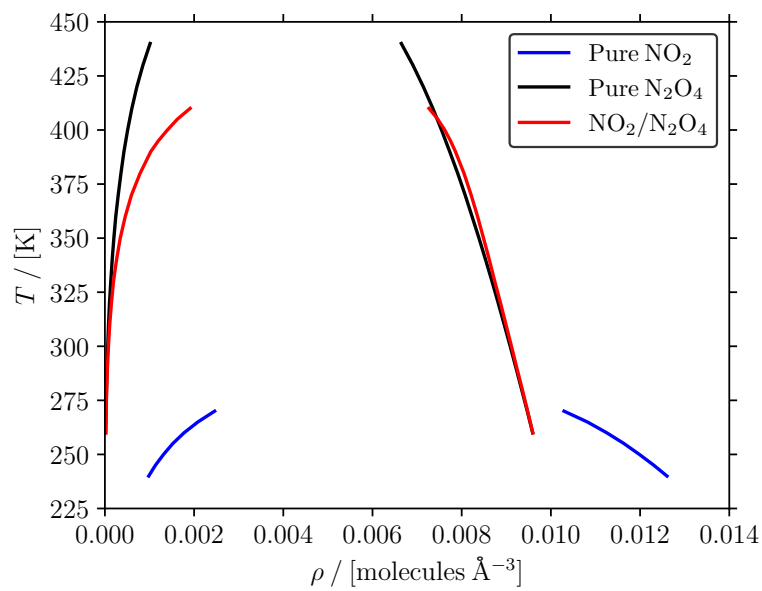


Figure S6: Computed densities of pure  $\text{NO}_2$ , pure  $\text{N}_2\text{O}_4$ , and the reactive mixture of  $\text{NO}_2$  and  $\text{N}_2\text{O}_4$  (system 1) as a function of temperature. For pure  $\text{NO}_2$  and pure  $\text{N}_2\text{O}_4$ , GEMC simulations were used, while for the reactive mixture of  $\text{NO}_2$  and  $\text{N}_2\text{O}_4$ , RE/GEMC simulations were used (including reaction R1 of the main text).

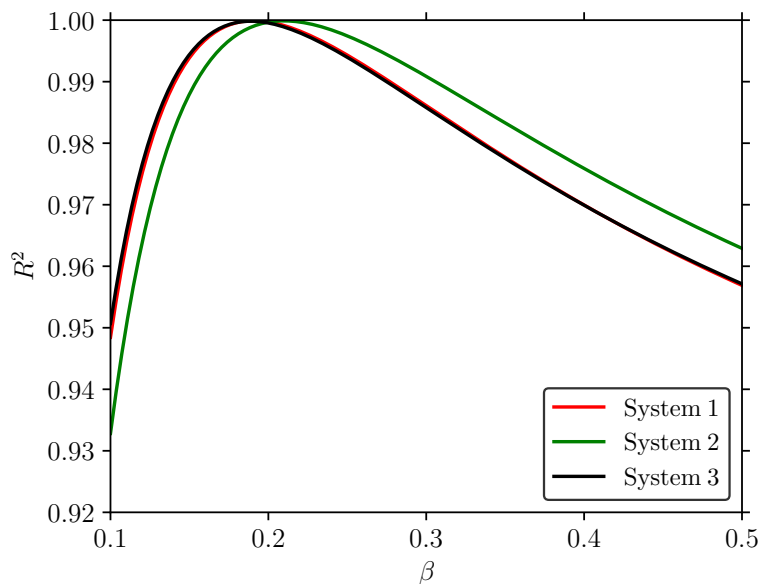


Figure S7: Coefficients of determination ( $R^2$ ) as a function of  $\beta$  for linear regression fits of the values of  $\left(\frac{\rho_1 - \rho_E}{\rho_0}\right)^{\frac{1}{\beta}}$  computed as a function of temperature with different force field parameters for the reactive  $\text{NO}_2/\text{N}_2\text{O}_4$  (A/A<sub>2</sub>) systems. See Table 2 of the main text for the force field parameters and Table S1 of the Supporting Information for the values of isolated molecule partition functions of monomers and dimers for different systems.

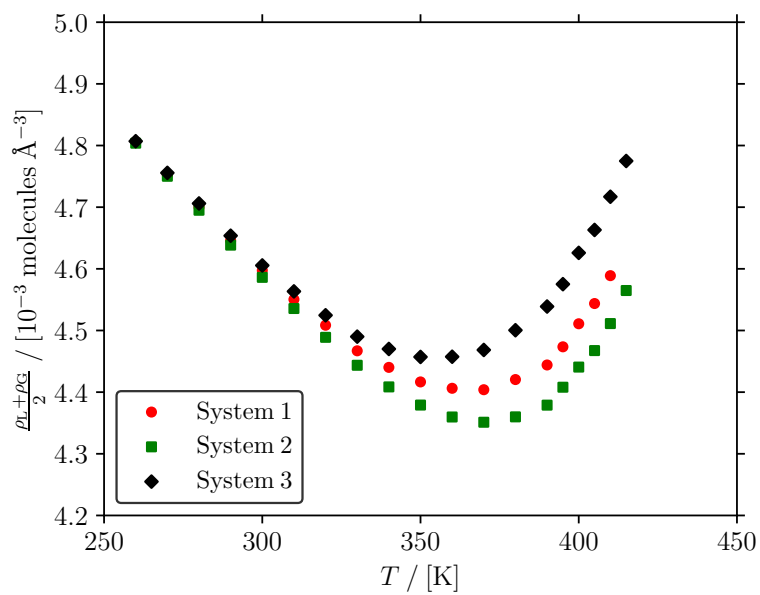


Figure S8: Average number densities of the liquid and gas phases computed using different force fields as shown in Table 2 of the main text with reaction R1 of the main text. See Table 2 of the main text for the force field parameters used in systems 1, 2, and 3.



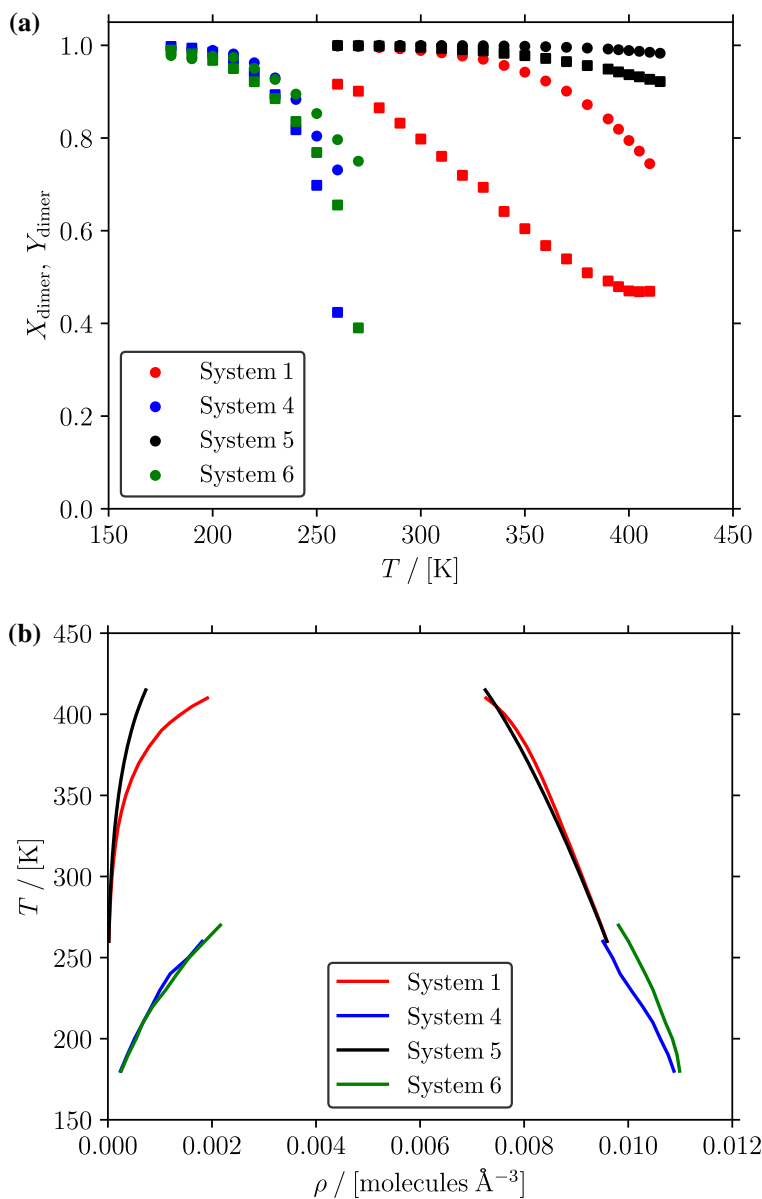


Figure S9: (a) Mole fractions of dimers in the gas (squares,  $Y_{\text{dimer}}$ ) and liquid (circles,  $X_{\text{dimer}}$ ) phases and (b) coexistence densities computed for different values of isolated molecule partition functions for dimers as a function of temperature. In our RE/GEMC simulations, the chemical reaction R1 is included. See Table 2 of the main text for the force field parameters and Tables S1-S4 of the Supporting Information for the values of isolated molecule partition functions of monomers and dimers for different systems.

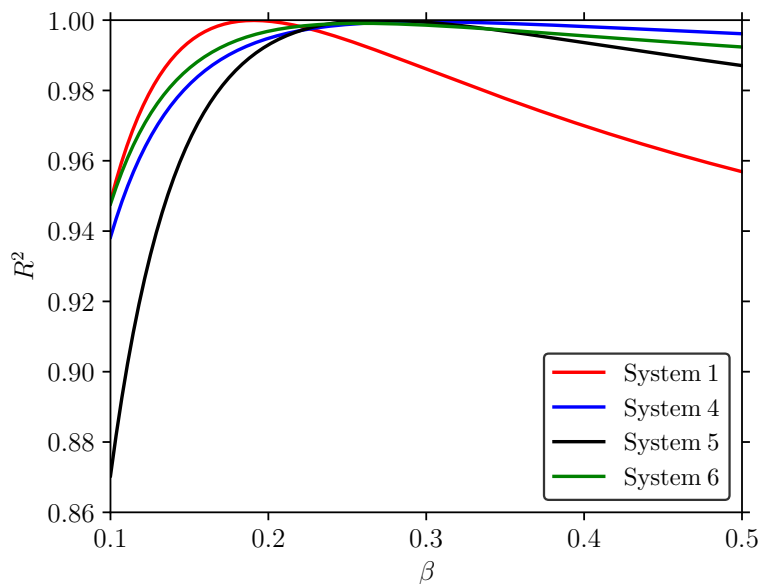


Figure S10: Coefficients of determination ( $R^2$ ) as a function of the critical exponent  $\beta$  for linear regression fits of the values of  $\left(\frac{\rho_1 - \rho_g}{\rho_0}\right)^{\frac{1}{\beta}}$  as a function of temperature with different values of isolated molecule partition function for dimers in reactive  $\text{NO}_2/\text{N}_2\text{O}_4$  ( $A/A_2$ ) systems. See Table 2 of the main text for the force field parameters and Tables S1-S4 of the Supporting Information for the values of isolated molecule partition functions of monomers and dimers for different systems.

## References

- [1] S. Lasala, K. Samukov, H. M. Polat, V. Lachet, O. Herbinet, R. Privat, J.-N. Jaubert, O. A. Moulton, K. D. Ras, T. J. H. Vlucht, Application of thermodynamics at different scales to describe the behaviour of fast reacting binary mixtures in vapour-liquid equilibrium, *Chemical Engineering Journal* 483 (2024) 148961.
- [2] H. H. Reamer, B. H. Sage, Volumetric behavior of nitrogen dioxide in the liquid phase, *Industrial & Engineering Chemistry* 44 (1952) 185–187.
- [3] A. Mittasch, E. Kuss, H. Schlueter, Dichten und dampfdrucke von wäßrigen ammoniaklösungen und von flüssigem stickstofftetroxyd für das temperatur-gebiet 0° bis 60°, *Zeitschrift für anorganische und allgemeine Chemie* 159 (1927) 1–36.